https://doi.org/10.1016/j.enggeo.2019.105322

A new simplified method for calculating consolidation settlement of multi-layer soft soils with creep under multi-stage ramp loading

by

Wei-Qiang FENG (Post-doctoral Fellow)
Department of Civil and Environmental Engineering
The Hong Kong Polytechnic University, Hung Hom, Kowloon, Hong Kong, China
Email: wqfeng@polyu.edu.hk

Jian-Hua YIN* (Chair Professor)
(Corresponding author)
Department of Civil and Environmental Engineering
The Hong Kong Polytechnic University, Hung Hom, Kowloon, Hong Kong.
Tel: (852) 2766-6065, Fax: (852) 2334-6389, Email: cejhyin@polyu.edu.hk

Wen-Bo CHEN (Ph.D.)
Department of Civil and Environmental Engineering
The Hong Kong Polytechnic University, Hung Hom, Kowloon, Hong Kong, China
Email: wenbo.chen@connect.polyu.hk

Dao-Yuan TAN (Ph.D.)
Department of Civil and Environmental Engineering
The Hong Kong Polytechnic University, Hung Hom, Kowloon, Hong Kong, China
Email: 14900443r@connect.polyu.hk

Pei-Chen WU (Ph.D. Candidate)
Department of Civil and Environmental Engineering
The Hong Kong Polytechnic University, Hung Hom, Kowloon, Hong Kong, China
Email: 16900045r@connect.polyu.hk

Manuscript submitted to *Engineering Geology* for possible publication as an Article
Sep. 2019

Abstract:

In normal practice, a multi-stage surcharge loading is applied gradually to achieve a certain strength of soft soils, and thus it is important to study the settlement of soft soils under multi-stage ramp loading. In this study, a new simplified method is developed to calculate the settlement of multi-layer soft soils exhibiting creep subjected to the multi-stage loading under a one-dimensional straining condition. The Zhu and Yin method is utilized to obtain the average degree of consolidation for multi-layer soils under each loading stage. The effects of creep compression on excess pore water pressure and total settlement during consolidation stage are elaborated. Subsequently, two typical projects, *Skå-Edeby* with 46 years' recorded settlement data and highway embankment in the *Berthierville* area, are selected as the typical multi-layer soil profiles. Cases with three different loadings and two different over consolidation ratio (OCR) values are analyzed using the finite element modeling, namely the new simplified method, and the Hypothesis A method. With the use of the results from finite element analysis as the reference, the new simplified method offers a good estimation of the settlement for all the cases and outperforms the Hypothesis A method in terms of accuracy.

Keywords: creep, simplified method, Hypothesis B, multi-stage loading, multi-layer soils

1. Introduction

With the rapid development of coastal areas, land reclamation has been increasing over the past five decades owing to the scarcity of land. The reclamation may lead to geotechnical problems such as large long-term settlement and the development of mud waves (Lai et al., 2019; Ersoy et al., 2019). Additional fills are placed on the seabed, that typically consists of layered soils with variable thicknesses. Thus, a reliable calculation method is required to estimate the total settlement after applying surcharge loadings in reclamation projects.

In practice, additional fills are surcharged gradually and incrementally with time. In many cases, the staged loading would be maintained over a period; the next staged loading is applied and maintained subsequently. This process is termed as multi-stage ramp loading (Lei et al., 2015). By assuming that the loading is applied uniformly over the construction period, an empirical method with a correcting factor on the instantaneous time-settlement curve was proposed by Terzaghi (1943) to consider the construction period effect. A mathematical equation was derived for the one-dimensional (1-D) consolidation of homogeneous soils under a ramp loading (Olson and Roy, 1977). Subsequently, an analytical solution for double-layered soil under a time-dependent loading was presented by Zhu and Yin (1999; 2005). The multi-stage ramp loading has brought to researchers' attentions such as Walker and Indraratna, (2009), Lei et al., (2015), Ai et al. (2019).

Taylor and Merchant (1940) first combined creep and consolidation mathematically. Subsequently, Taylor (1942) presented "Theory A" and "Theory B" to consider the secondary compression of soil behavior. Ladd et al. (1977) raised a fundamental question whether the creep acts as a separate phenomenon while excess pore water pressures dissipate during primary consolidation, leading to two possible extreme opinions in term of Hypotheses A and

B. Hypothesis A assumes that there is an identical EOP (end of primary) void ratio-effective vertical stress for laboratory specimen and in situ condition, whereas Hypothesis B assumes an EOP void ratio-effective vertical stress is dependent on the duration of primary consolidation and creep occurs during the “primary” consolidation. Many researchers advocated that the creep rate is only related to the current effective stress and strain state (Yin and Graham, 1996; Vermeer and Neher, 1999; Kim and Leroueil, 2001; Nash and Ryde, 2001; Degago et al., 2011, Yin et al., 2011, 2017), who all advocated Hypothesis B. On the contrary, other researchers supported that the creep occurs after the “primary” consolidation regardless the thickness scale (Mesri and Choi, 1985; Mesri and Vardhanabhuti, 2006), who advocated Hypothesis A. Bjerrum (1967) proposed the time line model with the concept of “instant compression” and “delayed compression” to interpret the compression of clays exhibiting creep. Subsequently, Garlanger (1972) developed the time line model proposed by Bjerrum (1967). The work of Garlanger (1972) was a large step forward at that time but has little or no application in practice as pointed out by Den Haan (2008). Yin and Graham (1996) analyzed the consolidation behavior of clays with different thicknesses in the 1-D straining condition by incorporating the elastic visco-plastic (EVP) model into the consolidation equation. Degago et al. (2011) reviewed the experimental investigations from previous literature to critically access the effect of creep during the consolidation phase, and it was found that the measured time-dependent compression of clays exhibits a good agreement with Hypothesis B.

In Hypothesis B, researchers have conducted numerous studies to investigate the coupling of creep and consolidation in the 1-D straining condition. Yin et al. (1994) first incorporated an EVP constitutive model into the consolidation equation and successfully simulated the anticipated porewater pressure. Yin and Zhu (1999) studied the mechanism of pore water pressure response in consolidation analysis of clayey soils in Tarsiut Island by implementing the EVP constitutive model into a finite element (FE) program; they found that the rising excess pore water pressure phenomenon of clays in the 1-D straining condition is caused by creep compression. Similar finding was identified by Stolle et al. (1999). Yuan and Whittle (2018) explained the increase in excess pore water pressure is due to the inconsistency between the total strain rate and visco-plastic strain rate.

Recently, Yin and Feng (2017) proposed a new approximate calculation method based on Hypothesis B for the settlement of soils including consolidation and creep based on the constitutive relationship of EVP and the "equivalent time" concept (Bjerrum, 1967; Yin and Graham, 1989; 1994). It has been verified that this new simplified method can be used in the calculation of soil layer under both instant loading and ramp loading by utilizing suitable solutions for obtaining the average degree of consolidation. However, this approach is only suitable for one-stage loading considered in the previous work (Yin and Feng, 2017; Feng and Yin, 2017, 2018) and it has not been validated in cases with multi-layer soft soils under a general multi-stage loading condition.

In this study, a new simplified calculation method is developed to calculate the consolidation settlement for multi-layer soft soils exhibiting obvious creep under a general multi-stage loading. The soft soils at both the normally consolidated state and over-consolidated state are considered in this approach by the "equivalent time" concept (Bjerrum, 1967; Yin and Graham, 1989; 1994). The soil profiles of the *Skå-Edeby* area and *Berthierville* area were utilized, and the measured settlements in the field are compared with the FE simulations and calculation results from this new simplified method. Subsequently, parametric studies including the different stress–strain states (over-consolidation ratio, *OCR* = 1.1 and 2), different staged loadings (one-, two-, and three-staged loadings), and different durations of one staged loading are conducted using the FE modeling and the new calculation method. The accuracy is also to be analyzed to illustrate the feasibility of this new simplified method for calculating the consolidation settlement of the multi-layer soft soils under a multi-stage ramp loading.

2. New Simplified Method for Multi-layer Soils Exhibiting Creep under Multi-stage Ramp Loading

In this study, a general multi-stage loading is shown in Figure 1. The construction period for each loading is denoted as t_{c1}, $t_{c2}, t_{c3}\ldots$, and the consolidation duration of each loading is expressed as t_1, t_2, $t_3\ldots$. These symbols will be used in the following equations and expressions.

For the multi-layer soils, *j* is the stage number of the loading and *i* is the layer number. It is regarded that the dissipation of excess pore water pressure under the *j*-th loading has no influence on the following excess pore water pressure dissipation of *j+1*-th loading. Thus, a general equation of this new simplified method based on Hypothesis B for the 1-D consolidation settlement of clayey soils under multi-stage loading can be expressed as

$$\begin{aligned} S_{totalB} &= \sum_{j=1}^{m}\left(S_{consolidation,j} + S_{creep,j}\right) \\ &= \sum_{j=1}^{m}\left\{U_{a,j}S_{consolidation,fj} + \left(\alpha S_{creep,fj} + (1-\alpha)S_{creep,dj}\right)\right\} \end{aligned} \tag{1}$$

where S_{totalB} is the total settlement ("*B*" implies that this approach is based on Hypothesis B); $S_{consolidation,j}$ is the consolidation settlement of multi-layer soils under *j*-th loading, $S_{consolidation,j} = U_{a,j}\sum_{j=1}^{n} S_{consolidation,fj}$; $S_{creep,j}$ is the creep compression of multi-layer soils under the j-th loading, that can be calculated as $S_{creep,j} = \sum_{j=1}^{n}\left(\alpha S_{creep,fj} + (1-\alpha)S_{creep,dj}\right)$; $S_{creep,fj}$ is the creep settlement with respect to the final j-th effective stress ignoring the coupling of the excess pore water pressure; $S_{creep,dj}$ is the delayed creep settlement due to the coupling of the excess pore water pressure; α is a parameter for calculating the creep settlement, whose value is in the range of 0–1. The details of α will be presented in following sections. In this method, the soil layers should first be divided into sublayer soils, as displayed in Figure 2. The calculation of the average degree of consolidation, the final settlement owing to the applied loading, and the creep settlement for each staged loading will be presented. In particular, the parameter α in the creep compression is discussed and interpreted.

2.1 Equations of Consolidation Settlement for Multiple Staged Ramp Loading

The final settlement, $S_{consolidation,fj}$, of the multi-layer soil under the j-th loading is calculated from the nonlinear stress–strain relationship of each subsoil layer:

$$S_{consolidation,fj} = \sum_{k=1}\left(\varepsilon_{fj,k}\right)h_k \tag{2}$$

where $\varepsilon_{fj,k}$ is the final strain of each sublayer under the j-th loading; h_k is the thickness of each sublayer. It should be noted that the thickness of each sublayer should be less than 0.5 m to obtain the accurate result because the initial vertical effective stress is variable with the depth and the stress–strain relationship of soft soil is nonlinear.

As shown in Figure 3, Point 0 is the initial stress–strain state, and Point 1 is the location of the stress–strain state after the first staged loading, similarly for Point 2 and Point 3. The compression data in Figure 3 are typically obtained from oedometer tests with loading, unloading, reloading stages. The duration of each compression loading is normally 24 hours

(1 day). Generally, we present the progress of the final strain calculation of each sublayer under the j-th loading.

(a) *Final Strain Calculation in j-th Loading*

For the sublayer of soil, when the final effective stress after the staged loading is located on the over-consolidated line (from Point 0 to Point 1, j = 1 in Figure 3), the final strain is calculated as

$$\varepsilon_{fj,k} = \frac{C_e}{(1+e_o)} \log\left(\frac{\sigma'_{zj,k}}{\sigma'_{z(j-1),k}}\right) \quad (3)$$

where $C_e/(1+e_0)$ is the slope of the over-consolidated line; e_o is the initial void ratio; $\sigma'_{zj,k}$ is the final effective stress after j-th loading of sublayer soil; $\sigma'_{z(j-1),k}$ the effective stress before the j-th loading.

When the final effective stress after the j-th staged loading is on the normally consolidated line (*e.g.*, from Point 1 to Point 2, from Point 2 to Point 3, in Figure 3), the final strain is obtained from the final stress-strain state with respect to the pre-consolidation pressure, expressed as

$$\varepsilon_{fj,k} = \frac{C_e}{(1+e_o)} \log\left(\frac{\sigma'_{zp(j-1),k}}{\sigma'_{z(j-1),k}}\right) + \frac{C_c}{(1+e_o)} \log\left(\frac{\sigma'_{zj,k}}{\sigma'_{zp(j-1),k}}\right) \quad (4)$$

where $C_c/(1+e_0)$ is the slope of the normally consolidated line; $\sigma'_{zp(j-1),k}$ is the pre-consolidation pressure before the j-th loading of sublayer soil, which is normally known for one stage loading. However, the pre-consolidation pressure in multi-stage loading is influenced by the effective stress before the j-th loading, $\sigma'_{z(j-1),k}$, expressed as

$$\sigma'_{zp(j-1),k} = 10^{\{\varepsilon_{z(j-2),t1,k} - \varepsilon_{zp(j-2),k}\}\frac{(1+e_o)}{(C_c-C_e)}} \times \left(\sigma'_{z(j-1),k}\right)^{-\frac{C_e}{(C_c-C_e)}} \times {\sigma'_{zp(j-2),k}}^{\frac{C_c}{(C_c-C_e)}} \quad (5)$$

It should be noted that the pre-consolidation pressure in the *j*-th loading is affected by the effective stress-strain state before *j*-th loading, detailed derivation is in the following part. Eq. (5) should be carefully used otherwise this approach would be obviously overestimate the total settlement.

The coefficient of volume compressibility of each soil layer, $m_{vj,i}$, is defined to describe the change per unit volume with respect to the increase in the *j*-th applied effective stress

$$m_{vj,i} = \frac{1}{n}\sum_{k=1}^{n}\frac{\left(\varepsilon_{fj,k} - \varepsilon_{f(j-1),k}\right)}{\left(\sigma'_{zj,k} - \sigma'_{z(j-1),k}\right)} \tag{6}$$

The coefficient of consolidation of each soil layer is calculated as

$$c_{vj,i} = \frac{k_{z,i}}{\gamma_w m_{vj,i}} \tag{7}$$

where $k_{z,i}$ is the hydraulic conductivity of each soil layer, and γ_w is the unit weight of water, taken as *10 kN/m³*.

(b) Average Degree of Consolidation of Multiple Soil Layers

To analyze the consolidation settlement, the average degree of consolidation of multi-layer soils must be determined. Feng and Yin (2017) examined the consolidation performance in the new simplified method of double–layered soil under a time-dependent loading. The Zhu and Yin method (1999, 2005) was recommended in the calculation of the average degree of consolidation. Thus, this method is utilized in this study for calculating the average degree of consolidation of multiple soil layers under each stage loading.

For the *j*-th loading, the average degree of consolidation ($U_{a,j}$) is calculated as

$$U_{a,j}\left(T_j,T_{c,j}\right)=\begin{cases}\dfrac{T_j}{T_{c,j}}-\sum_{n=1}^{\infty}\dfrac{c_{n,j}}{\lambda_n^4 T_{c,j}}\left[1-\exp\left(-\lambda_{n,j}^2 T_j\right)\right] & T_j \le T_{c,j}\\ 1-\sum_{n=1}^{\infty}\dfrac{c_{n,j}}{\lambda_{n,j}^4 T_{c,j}}\left[1-\exp\left(-\lambda_{n,j}^2 T_{c,j}\right)\right]\times\exp\left[-\lambda_{n,j}^2\left(T_j-T_{c,j}\right)\right] & T_j > T_{c,j}\end{cases} \tag{8}$$

where T_j is the normalized time factor; $T_j=\dfrac{c_{vj,1}c_{vj,2}t}{\left(H_1\sqrt{c_{vj,2}}+H_2\sqrt{c_{vj,1}}\right)^2}$; $T_{c,j}$ is the normalized construction time factor; $T_{c,j}=\dfrac{c_{vj,1}c_{vj,2}t_c}{\left(H_1\sqrt{c_{vj,2}}+H_2\sqrt{c_{vj,1}}\right)^2}$; $\lambda_{n,j}$ is the equation root of $sin\theta+p_j sin(q_j\theta)=0$ for the double–drained condition including the top and bottom (termed as *condition1*), and $cos\theta-p_j cos(q_j\theta)=0$ for the one–drained condition (termed as *condition2*). $c_{n,j}$ is obtained from the following expressions

$$c_{n,j}=\begin{cases}\dfrac{2\left[m_{vj,1}H_1\xi_j sin(\lambda_{n,j}\xi)+m_{vj,2}H_2\xi_j sin(\lambda_{n,j}\xi)\right]^2}{\omega_j^2\xi_j^2\left(m_{vj,1}H_1+m_{vj,2}H_2\right)\left[m_{vj,1}H_1\xi_j sin^2(\lambda_{n,j}\xi_j)+m_{vj,2}H_2\xi sin^2(\lambda_{n,j}\xi_j)\right]} & for\ condition1\\ \dfrac{2\left[m_{vj,1}H_1\xi_j cos(\lambda_{n,j}\xi_j)\right]^2}{\omega_j^2\left(m_{vj,1}H_1+m_{vj,2}H_2\right)\left[m_{vj,1}H_1\xi_j cos^2(\lambda_{n,j}\xi_j)+m_{vj,2}H_2\xi_j sin^2(\lambda_{n,j}\xi_j)\right]} & for\ condition2\end{cases} \tag{9}$$

where

$$p_j=\frac{\sqrt{k_2 m_{vj,2}}-\sqrt{k_1 m_{vj,1}}}{\sqrt{k_2 m_{vj,2}}+\sqrt{k_1 m_{vj,1}}}$$

$$q_j=\frac{H_1\sqrt{c_{vj,2}}-H_2\sqrt{c_{vj,1}}}{H_1\sqrt{c_{vj,2}}+H_2\sqrt{c_{vj,1}}}$$

$$\omega_j=(1+q_j)/2$$

$$\xi_j=(1-q_j)/2$$

The details of the derivation could be found in Zhu and Yin (1999; 2005).

2.2 Equations of Creep Settlement for Multiple Staged Loading

The creep settlement after the j-th loading is calculated using the following equations

$$S_{creep,fj} = \sum_{k=1} \left(\varepsilon_{creep,fj,k} \right) h_k \tag{10}$$

$$S_{creep,dj} = \sum_{k=1} \left(\varepsilon_{creep,dj,k} \right) h_k \tag{11}$$

where $\varepsilon_{creep,fj}$ is the creep strain with respect to the final effective stress under the j-th loading ignoring the coupling of the excess pore water pressure; $\varepsilon_{creep,dj}$ is the delayed creep strain under the j-th loading due to the coupling of the excess pore water pressure. “Delayed creep strain” implies that the creep strain is influenced by the dissipation of excess pore water pressure in the field.

As shown in Figure 3, a family of equivalent time lines represents different creep strain rates. Following the assumptions of the EVP constitutive model, the creep strain rate is independent of the stress path. When the final effective stress after the staged loading of each sublayer soil is on the over-consolidated line (for example, from Point 0 to Point 1 in Figure 3), the final creep strain is obtained as

$$\varepsilon_{creep,fj,k} = \frac{C_{\alpha e}}{\left(1+e_o\right)} \log\left(\frac{t_o + t_{ej,k}}{t_o + \Delta t_{ej,k}} \right) \tag{12}$$

where $C_{\alpha e,j}$ is the creep coefficient of soil layer, whose value is the slope of $e-\log(t)$ after the time of t_o obtained from the oedometer test results; t_o is the creep parameter in units of time, $t_o = 1\ day$ in this study; $\Delta t_{ej,k}$ and $t_{ej,k}$ are the calculated “equivalent time” based on the assumption that the change in strain is stress–path independent when t is larger than $t_{cj}/2$ from the following equations

$$\Delta t_{ej,i} = t_o \times 10^{\left(\left(\varepsilon_{fj,k} - \varepsilon_{zp(j-1),k} \right) \frac{(1+e_0)}{C_{\alpha e}} \right)} \left(\frac{\sigma'_{zj,k}}{\sigma'_{zp(j-1),k}} \right)^{-\frac{C_c}{C_{\alpha e}}} - t_o \tag{13}$$

$$t_{ej,k} = t - \sum_{j=1}^{j-1} t_j - \frac{t_{cj}}{2} - t_o + \Delta t_{ej,k} \tag{14}$$

For the sublayer soil is at the normally consolidated state, the final creep strain is calculated as

$$\varepsilon_{creep,fj,k} = \frac{C_{\alpha e}}{(1+e_o)} \log\left(\frac{t_o + t_{ej,k}}{t_o}\right) \tag{15}$$

$$t_{ej,k} = t - \sum_{j=1}^{j-1} t_j - \frac{t_{cj}}{2} - t_o \tag{16}$$

The delayed creep settlement, $\varepsilon_{creep,dj}$, is similar to the $\varepsilon_{creep,fj}$ in all cases mentioned above but delayed by the time of $t_{EOP,field}$. For the sublayer soil at the over-consolidated state, the delayed creep strain is calculated as

$$\varepsilon_{creep,dj,k} = \frac{C_{\alpha e}}{(1+\mathrm{e}_o)} \log\left(\frac{t_o + t_{ej,k}}{\Delta t_{ej,k} + t_{EOP,field}}\right) \tag{17}$$

Similarly, the delayed creep strain of the subsoil at the normally consolidated state is obtained as

$$\varepsilon_{creep,dj,k} = \frac{C_{\alpha e}}{(1+e_o)} \log\left(\frac{t_o + t_{ej,k}}{t_{EOP,field}}\right) \tag{18}$$

Eq. (18) is the same as the "secondary consolidation" strain in the traditional Hypothesis A method when the soil layer is under an instant loading, as presented in Yin and Feng (2017). However, this delayed creep strain can also be used in the over-consolidated state in the new simplified calculation method with the same creep parameter and "equivalent time," whereas a new value of the "secondary consolidation" coefficient is defined in the traditional Hypothesis A method for the soil at the over-consolidated state (Feng and Yin, 2018).

2.3 Elaboration of Parameter α in Creep Settlement

In Eq. (1), α is a paramount parameter to evaluate the displayed creep settlement during the consolidation stage. As reported by Yin and Feng (2017), a highly partial differential equation must be established for the consolidation problems of clayey soils exhibiting creep

$$\frac{k_z}{\gamma_w}\frac{\partial^2 u_e}{\partial z^2}=\frac{C_e}{\left(1+e_o\right)\ln(10)}\frac{\partial u_e}{\partial t}-\frac{C_{\alpha e}}{\left(1+e_o\right)\ln(10)t_o}10^{-\left(\left(\varepsilon_{fj,k}-\varepsilon_{zp(j-1),k}\right)\frac{(1+e_0)}{C_{\alpha e}}\right)}\left(\frac{\sigma_{zj,k}-u_e}{\sigma'_{zp(j-1),k}}\right)^{\frac{C_c}{C_{\alpha e}}} \tag{19}$$

where $u_{e,j}$ is the excess pore water pressure of the *j*-th loading. Eq. (19) is a fully coupled equation that considers the loading conditions and loading histories (Yin and Graham, 1996). Using the average value of the nonlinear compressibility and adopting Terzaghi's theory, the coupled equation is simplified as

$$\frac{k_z}{\gamma_w}\frac{\partial^2 u_e}{\partial z^2}=\left\{\frac{1}{n}\sum_{i=1}^{n}\frac{\left(\varepsilon_{fj,i}-\varepsilon_{f(j-1),i}\right)}{\left(\sigma'_{zj,i}-\sigma'_{z(j-1),i}\right)}\right\}^{-1}\frac{\partial u_e}{\partial t} \tag{20}$$

The influence of creep compression during the consolidation stage is neglected. Thus, α is adopted as the parameter to evaluate the expressed creep settlement during the consolidation stage. When the soil layer is within 10 m, $\alpha = 0.8$ is suggested (Yin and Feng, 2017; Feng and Yin, 2018). However, this simplification may overestimate the creep compression during the early stage of the consolidation of thick soil layer (*e.g.* thicker than 10 m).

The creep effect can be investigated directly by comparing the results of FE simulations with two different values of the creep parameter. The typical parameter values of the Hong Kong Marine Deposits (HKMD) are listed in Table 1. The FE model was established with a 10–m soil layer with a surcharge of 30 kPa. The top is drain and the bottom is impermeable. A series of points are pre-set in the FE simulation to monitor the ground settlement and excess pore water pressure of soil layer. The details of the finite element simulation can be referred in Yin and Feng (2017). All parameters are the same except the creep coefficient in the finite element simulation (two different values of μ^* in Table 1), thus, the difference of simulated results is only influenced by the creep coefficient (Yin et al., 2011). The simulated results are compared to interpret the creep effect on the consolidation settlement and excess pore water pressure during and after consolidation.

As illustrated in Figure 4, an obvious difference occurs in the excess pore water pressure response and the settlement of the soil layer. For the soil layer, the creep effect is reserved in the excess pore water pressure initially, as displayed in Figure 4(a), subsequently, it is expressed in the surface settlement gradually, which can be observed by engineers. Therefore, the parameter α is a variable related to the average degree of consolidation rather than a constant. In this study, we use $\alpha = U_{a,j}$ as a simplification.

2.4 Determination of Pre-consolidation Pressure in the j-th Loading

As mentioned above, the pre-consolidation pressure in the *j*-th loading, which is directly related to the total settlement in the calculation, is affected by the effective stress-strain state before the *j*-th loading and should be carefully determined. As illustrated in Figure 3, the pre-consolidation pressure of each sublayer at normal-consolidated state used in stage 3 is derived as:

$$\begin{aligned}
&\varepsilon_{zp2,k} = \varepsilon_{z2,t2,k} + C_e/V \log\left(\frac{\sigma'_{zp2,k}}{\sigma'_{z2,k}}\right) = \varepsilon_{zp,k} + C_c/V \log\left(\frac{\sigma'_{zp2,k}}{\sigma'_{zp,k}}\right) \\
&\varepsilon_{z2,t2,k} - \varepsilon_{zp,k} = C_c/V \log\left(\frac{\sigma'_{zp2,k}}{\sigma'_{zp,k}}\right) - C_e/V \log\left(\frac{\sigma'_{zp2,k}}{\sigma'_{z2,k}}\right) \\
&\varepsilon_{z2,t2,k} - \varepsilon_{zp,k} = \left\{C_c/V - C_e/V\right\} \log\left(\sigma'_{zp2,k}\right) - C_c/V \log\left(\sigma'_{zp,k}\right) + C_e/V \log\left(\sigma'_{z2,k}\right) \\
&\log\left(\sigma'_{zp2,k}\right) = \left\{\varepsilon_{z2,t2,k} - \varepsilon_{zp,k}\right\} \frac{V}{\left(C_c - C_e\right)} + \frac{C_c}{\left(C_c - C_e\right)} \log\left(\sigma'_{zp,k}\right) - \frac{C_e}{\left(C_c - C_e\right)} \log\left(\sigma'_{z2,k}\right)
\end{aligned}$$

Thus, the new pre-consolidation pressure in stage 3 can be obtained as

$$\sigma'_{zp2,k} = 10^{\left\{\varepsilon_{z2,t2,k} - \varepsilon_{zp,k}\right\}\frac{V}{(C_c - C_e)}} \times \left(\sigma'_{z2,k}\right)^{-\frac{C_e}{(C_c - C_e)}} \times \sigma'^{\frac{C_c}{(C_c - C_e)}}_{zp,k} \tag{21}$$

Similarly, this derivation process is also valid for the sublayer soil at over-consolidated state.

Eq. (21) could be extended to the *j*-th staged loading, expressed as

$$\sigma'_{zp(j-1),k} = 10^{\left\{\varepsilon_{z(j-2),t1,k} - \varepsilon_{zp(j-2),k}\right\}\frac{(1+e_o)}{(C_c - C_e)}} \times \left(\sigma'_{z(j-1),k}\right)^{-\frac{C_e}{(C_c - C_e)}} \times \sigma'_{zp(j-2),k}{}^{\frac{C_c}{(C_c - C_e)}} \tag{22}$$

2.5 Hypothesis A Method for Calculating the Settlement of Multiple Soil Layers

Hypothesis A method is also presented in this study to calculate the total consolidation settlement in the field

$$\begin{aligned} S_{totalA} &= S_{"primary"} + S_{"secondary"} \\ &= \begin{cases} \sum_{j=1}^{m} U_{a,j} S_{fj} & \text{for } t \le t_{EOP,field} \\ \sum_{j=1}^{m} U_{a,j} S_{fj} + S_{"secondary",j} & \text{for } t > t_{EOP,field} \end{cases} \end{aligned} \tag{23}$$

where $S_{"primary",j}$ is the "primary" consolidation settlement under the *j*-th staged loading at time *t*, which is the same as $S_{consolidationj}$ in Eq. (7); $t_{EOP,field}$, which represents the end of the "primary" consolidation in the field, is the time when $U_a = 98\%$. $S_{"secondary",j}$ is the same as the calculation of the delayed creep settlement. However, the "secondary consolidation" settlement is not considered for the sublayers at the over-consolidated state.

3. Two Projects of Multiple Soil Layers Subjected to the Multi-ramp Loadings

3.1 Site Descriptions and Finite Element Modeling

(a) The Skå-Edeby Test Fill

Using the test fill of area IV as an example, the diameter is 35 m and the fill height is 1.5 m. Larsson and Mattsson (2003) introduced the total surcharge loading on the test fill surface of approximately 27 kPa. The loading was started from 1956 and finished within two months (60 days); subsequently, the filled loading was retained for 46 years. The settlements at different depths were also recorded. The total thickness of soft soil layer is 12 m, including a 2–m thick layer of desiccated dry crust on top, and the soft soils overlay on the bedrock. The subsoil composites of the recent and post-glacial clays of Central Sweden in the soil profile have been reported (Holtz and Broms, 1972). The test fill is approximately 2.5 m above the average sea level after emerging from the Baltic Sea 500 years ago. Perrone (1998) reported that the upper post-glacial layers to the recent top layers were deposited up to 4500 years, and the glacial clay layers were formed approximately 7500 years ago. Therefore, we divided the geological profile into multiple layers and the actual surcharge is the one-staged ramp loading.

(b) The highway embankment on Berthierville site

Samson and Garneau (1974) presented the construction of large embankments on the soft soils and monitored the settlements over a long period. The highway embankment was constructed between *Montreal* and *Berthierville.* The soil profile consists of normally consolidated stratified fluvial deposits with the thickness of 18 m overlying the highly over-consolidated marine clay. The settlement was monitored from 1964 to 1972 during and after construction. It was found that the major settlement occurred at the upper fluvial deposits (18 m) with normally consolidated state. There is no evidence of lateral plastic deformation in the monitoring area of the highway embankment, which indicates that this project could be regarded as 1-D straining condition. 17 Oedometer consolidation test samples were collected and six samples were taken from the upper fluvial deposits. The main parameters obtained from the oedometer consolidation test results are listed in Table 3(a), which is consistent with the data reported by Samson and Garneau (1974). Based on the data from boreholes, the typical geotechnical profile was plotted: the upper profile of 18 m is made up of silty fine sand (2.25 m), silty clay (9.75 m) and sandy silt (6 m). The groundwater level is 1 m below the silty fine sand surface. Because the foundation condition is very poor, the embankment was designed as staged construction with necessary consolidation period. The final height of sand fill is 10.7 m. The staged loading is plotted in Figure 5. The construction period of first staged loading is 40 days, then, the loading was maintained for six months. Afterwards, the second staged loading was gradually applied within 60 days and kept constant for the consolidation. The fill loading was calculated from the height of the sand fill (the unit weight of the sand fill is 18.2 kN/m^3). Detailed information could be found in Samson and Garneau (1974).

(c) Finite element modelling

As illustrated in Figure 6(a), a multi-layer geometry finite element model using the Plaxis software (2015 version) was analyzed based on the information mentioned above. For the *Skå-Edeby* test fill, the axis-symmetric model type was set to model the circular test fill. Three sublayers were simulated in the FE model using the SSC model, and the parameters of each sublayer are listed in Table 2, which are consistent with the data reported by Le (2015). The boundary conditions of the top and bottom were set as drained according to the geological condition. For Case 1, a one-staged ramp loading was considered; a two-staged ramp loading for Case 2, and a three-staged ramp loading for Case 3 were considered in the finite element simulations. The construction period for each stage loading is 60 days. The total duration was 36500 days to compare with the measured data in the field.

Similarly, the sublayers were computed using the FE model with the SSC model for the highway embankment on *Berthierville* site. According to the geology information, the top silty sand layer was set as drained condition, and the bottom was set as impermeable condition considering that the underlying soil is marine clay, as shown in Figure 6(b). All the parameters in the FE simulation are listed in Table 3(b). Two staged ramp loadings were applied based on the information of the construction. As a comparison, one longer duration of the first staged loading was considered to illustrate the influence of the duration on the consolidation of multi-layer soils under the subsequent loading.

3.2 *Calculation Procedures of New Simplified Method and Hypothesis A Method*

In this section, the procedures in the new simplified method and Hypothesis A method are presented. The soil layer is first divided into sublayer soils. The initial effective stress state of each sublayer is calculated based on the unit weight of soils and the depth in the middle of each sublayer. It should be noted that the unit weight of each soil layer may be different for the multi-layer soil condition.

The pre-consolidation pressure and final effective stress state under each staged loading are computed from the staged loading. The stress state of each sublayer is determined by comparing the final effective stress and pre-consolidation pressure. The consolidation strain under each staged loading is calculated by Eq. (3) for the sublayers at over-consolidated state and Eq. (4) for the sublayers at normally consolidated state. Regarding the top 6 m as layer 1, and the bottom 6m as layer 2, the soil profile of the *Skå-Edeby* site is a double–layered soil (as shown in Figure 6(a)). The average degree of consolidation is calculated by Zhu and Yin method (1999; 2005). Table 4 lists a summary of all calculated parameter values in Case 2 as a reference. Subsequently, the creep strain of each sublayer is also computed based on the stress state of the sublayers. The creep strain will remain at the constant value of $\varepsilon_{creep,tj,k}$ after the time becomes larger than t_j for the j-th loading. Finally, the total consolidation settlement is obtained by summing the consolidation settlement and creep compression under all the staged loadings, using Eq. (1). Similarly, the calculation procedures of *Berthierville* site were repeated and the main calculated parameters are listed in Table 5.

3.3 Comparison of the New Simplified Method, Finite Element Analysis, and Measured Data in the Field

In this section, the measured data from two projects is regarded as the standard to evaluate the performance of the FE analysis and the new simplified method for the *Skå-Edeby* fill and highway embankment in *Berthierville* site. The calculation results using the new simplified method and Hypothesis A method are compared with FE simulation results for all the cases described above. The *relative error* ($\xi_{totalB,t}$) is utilized to assess the accuracy of the new simplified method with the FE results:

$$\xi_{totalB,t} = \frac{\left|S_{totalB,t} - S_{FE,t}\right|}{S_{FE,t}} \times 100\% \tag{24}$$

where $S_{totalB,t}$ is the calculated result from the new simplified method at a certain time; $S_{FE,t}$ is the results from finite element modelling. $\xi_{totalA,t}$ is similarly defined to examine the accuracy of the simple method based on Hypothesis A.

3.3.1 Validation of Finite Element Results and Measured Settlements

Figure 7 displays the comparison of the measured settlements at different depths, and the FE simulation results of soil profile in the *Skå-Edeby* subjected to a ramp loading.

It is observed that the FE simulation results show a good agreement with the settlement measured in the field at different depths. In the FE simulation, the settlement at 0 m after construction (60 days) is 0.068 m, close to the field measurement of 0.045 m (Larsson and Mattsson, 2003). In addition, the total settlement at the surface after 46 years in the FE analysis is 1.151 m, and the measured settlement in the field is 1.102 m. Thus, the good agreement between the results from FE simulation and measured data in the field provides the evidence that the parameter values for each soil layer listed in Table 2 are representative.

Similarly, the comparison of the measured settlements and the FE simulation results of highway embankment in *Berthierville* site subjected to two-stage ramp loading is plotted in Figure 8. The FE simulated settlement agrees well with the measured data in the site. It confirms that the parameter values in the FE modelling are reasonable.

3.3.2 Verification of the New Simplified Method for Different Staged Loadings

(a) The Skå-Edeby Test Fill

Figure 9 shows the comparison of the calculated results from the new simplified method, FE simulation results, and measured settlement in the field subjected to three different staged loadings, termed as Case 1, Case 2, and Case 3. The construction period for each staged loading is 60 days. The consolidation duration of each loading is plotted in Figure 9.

For Case 1, the one-staged ramp loading of 27 kPa is applied, which is the applied loading in the field. The calculated settlement from the new simplified method is close to both the measured data and FE simulated result. The top 2 m is the crust layer, and the soil of this layer is at the over-consolidated state. Underneath the crust layer, soft layer 1 with 4 m thickness (OCR = 1.1) and soft layer 2 with 6 m thickness (OCR = 1) are at the normally consolidated state with the applied loading of 27 kPa. The good performance of the new simplified method indicates that the creep compression is reasonably considered during the consolidation. The *relative errors* of the new simplified method are calculated and shown in Figure 9. For Case 2, a two-staged ramp loading is accounted. The second stage loading of 27 kPa is applied after 10000 days. Before the 10000 days, the results from the new simplified method and FE simulations are the same as those in Case 1. Using the measured settlement as the reference, the effect of the second staged loading is shown clearly. It should be noted that the pre-consolidation pressure is updated using Eq. (5) for each sublayer. Most sublayers of the multiple soil profile are at the over-consolidated state in the stage 2 loading. Therefore, the creep compression is calculated using the "equivalent time" concept for each sublayer in stage 2 loading (Eqs. 12–14). For Case 3, the stage 1 loading in Case 2 is divided into a two-staged loading with each stage loading of 13.5 kPa. The obvious turning point is observed at the 1000-*th* day in the FE analysis. Again, the new simplified method captures this performance correctly. The computed settlement of this simplified method also agrees well with the simulation results from the Plaxis software. The measured data in Case 1 is attached to the figure to illustrate the influence of the applied loading. Thus, it is demonstrated that the new simplified method could accurately estimate the consolidation settlement of soil layers exhibiting creep subjected to a general loading condition.

Three loading cases are also examined with OCR = 2 for soil layer 1 and soil layer 2 underneath the crust layer. The calculated results are compared with the modeling results from the FE program, as plotted in Figure 10. It is shown that the new simplified method calculates the settlement close to the FE simulations of Plaxis for three loading conditions, thereby proving that this method could also consider the initial stress state of the soil layers. The initial stress state is closely related to the consolidation settlement of stage 1 loading. The values of the *relative error* for the new simplified method vary from 1.444% to 12.703%, which are acceptable for engineering applications (see Figure 10).

(b) The highway embankment in Berthierville site

Figure 11 shows the comparisons of calculated results, FE modelled results, and the measured data in the site subjected to two different staged loadings. It can be seen that the calculated results from the new simplified method are very close to the FE simulated results. It should be noted that the measured data in the field are also influenced by the combination of underlying marine soil layer and variable compressibility. The measured data from settlement gauge on the underlying marine clay with highly over-consolidated state illustrate the gradual increase of settlement from 1969, which induces a bit gap between the measured settlement and the FE simulated results. Thus, the accuracy of this new simplified method is evaluated by Eq. (24) based on the FE simulated results, whose value is listed on the figure. The relative error of the new simplified method varies from 2.6% to 7.5%.

Comparatively, under different staged loadings, the Hypothesis A method underestimated the total settlements for all three cases, and the values of *relative error* are plotted in Figures 9, 10 and 11, which are unacceptable. It should be noted that this new simplified method is only valid for one-dimensional straining condition, which is suitable for the large area project over multi-layer soils. In the literature, there are many reclamation projects with monitored settlements. However, it should be first examined that whether it could be regarded as 1-D straining condition. Normally, the width of the reclamation area should be more than three to five times of the thickness of the soil layer. The compressibility variation of the soft soils and the drainage boundary condition should be carefully considered. It is recommended that the new simplified method should be first used for the oedometer test results before the application in the real project.

4. Conclusions

In this study, we developed a new simplified method to calculate the settlements including both the consolidation and creep settlements of multi-layer soils subjected to a general multi-stage loading. The equations for calculating the consolidation and creep compression were presented. The average degree of consolidation (U_a) for multi-layer soils was computed using the Zhu and Yin method for each staged loading. An FE software using the SSC model was utilized to verify this new simplified method as well as the Hypothesis A method. The primary findings and conclusions are as follows:

(a) In the fully coupled analysis of consolidation and creep, the creep compression first induced the increase in the excess pore water pressure. Subsequently, it was displayed gradually in the total settlement with the dissipation of the induced excess porewater pressure by creep compression. Thus, $\alpha = U_a$ was utilized in the new simplified method to calculate the creep settlement.

(b) Area VI in the *Skå-Edeby* site and highway embankment in *Berthierville* site are typical multi-layer soil profiles in two typical drained conditions. The settlements from the FE simulations agreed well with the measured settlements in these two fields, thus confirming that the parameter values of each layer in the simulation were credible.

(c) With the soil profile of *Skå-Edeby* site, three different ramp loadings were considered. The results of this new simplified method were close to the FE modeling results with *relative errors* lower than 12.7%. Similar finding was obtained from the highway embankment in *Berthierville* site with the values of relative error less than 7.5%, which fully satisfied the requirement in engineering design.

(d) In this study, Hypothesis A method has yielded a pronounced error compared with the FE simulations in all the ramp loading cases when adopting the same values of parameters as those in the finite element modelling, even during the primary consolidation stages. Thus, Hypothesis A method is not suitable in determining the consolidation settlement of multi-layer soils exhibiting creep subjected to multi-stage loading.

Acknowledgement

The work in this paper is supported by a National State Key Project "973" grant (Grant No.: 2014CB047000) (sub-project No. 2014CB047001) from Ministry of Science and Technology of the People's Republic of China, a CRF project (Grant No.: PolyU 12/CRF/13E) from Research Grants Council (RGC) of Hong Kong Special Administrative Region Government (HKSARG) of China, two GRF projects (PolyU 152196/14E; PolyU 152796/16E) from RGC of HKSARG of China. The authors also acknowledge the financial supports from Research Institute for Sustainable Urban Development of The Hong Kong Polytechnic University, grants (1-ZVCR, 1-ZVEH, 4-BCAU, 4-BCAW, 5-ZDAF, G-YN97) from The Hong Kong Polytechnic University.

References

Ai, Z. Y., Zhao, Y. Z., Song, X., and Mu, J. J. 2019. Multi-dimensional consolidation analysis of transversely isotropic viscoelastic saturated soils. *Engineering Geology*, 253, 1-13.

Bjerrum, L., 1967. Engineering geology of Norwegian normally-consolidated marine clays as related to settlements of buildings. *Géotechnique*, 17(2), 83–118.

Degago, S. A., Grimstad, G., Jostad, H. P., Nordal, S., and Olsson, M. 2011. Use and misuse of the isotache concept with respect to creep hypotheses A and B. *Géotechnique*, 61(10), 897–908.

Den Haan, E. J. 2008. De intrinsieke tijd in het isotachenmodel. *GEOtechniek*, 1, 34–38.

Ersoy, H., Karahan, M., Babacan, A. E., and Sünnetci, M. O. 2019. A new approach to the effect of sample dimensions and measurement techniques on ultrasonic wave velocity. *Engineering Geology*, 251, 63-70.

Feng, W.-Q., and Yin, J.-H., 2017. A new simplified Hypothesis B method for calculating consolidation settlements of double soil layers exhibiting creep. *International Journal for Numerical and Analytical Methods in Geomechanics*, 41(6), 899–917.

Feng W.-Q., and Yin J.-H. 2018. A new simplified Hypothesis B method for calculating the consolidation settlement of ground improved by vertical drains. *Int. J. Numer. Anal. Methods Geomech.* 42, 295–311. https://doi.org/10.1002/nag.2743.

Garlanger, J. E. 1972. The consolidation of soils exhibiting creep under constant effective stress. *Géotechnique*, 22(1), 71–78.

Holtz, R.D. and Broms, B. 1972. Long-term loading tests at Ska-Edeby, Sweden. *Proceedings of the ASCE Specialty Conference on the Performance of Earth Supported Structures*, Purdue University, Lafayette, Indiana, 273–284.

Kim, Y. T. and Leroueil, S. 2001. Modeling the viscoplastic behavior of clays during consolidation: application to Berthierville clay in both laboratory and field conditions.

Can. Geotech. J. 38, No. 3, 484–497.

Ladd, C. C., Foott, R., Ishihara, K., Schlosser, F. and Poulos, H. G. 1977. Stress-deformation and strength characteristics. state-of the-art report. *Proc. 9th Int. Conf. Soil Mech. Found. Engng*, Tokyo 2, 421–494.

Lai, C. Y., Wong, L. N. Y., and Wallace, M. 2019. Review and assessment of In-situ rock stress in Hong Kong for territory-wide geological domains and depth profiling. *Engineering Geology*, 248, 267-282.

Larsson, R. and Mattsson, H. 2003. *Settlements and shear strength increase below embankments. Geotechnical Institute Report*, 63.

Le, T.M. 2015 Analysing consolidation data to optimise elastic visco-plastic model parameters for soft clay. Ph.D. thesis, University of Technology Sydney, Sydney, Australia.

Lei, G. H., Zheng Q., Ng C. W. W., Chiu A. C. F. and Xu B. 2015. An analytical solution for consolidation with vertical drains under multi-ramp loading. *Géotechnique*, 65(7), 531–547.

Mesri, G. and Choi, Y. K. 1985. The uniqueness of the end-of primary (EOP) void ratio-effective stress relationship. *Proc. 11th Int. Conf. Soil Mech. Found. Engng,* San. Francisco 2, 587–590.

Messi, G. and Vardhanabhuti, B. 2006. Closure of 'Secondary compression' by Mesri and Vardhanabhuti (2005). *J. Geotech. Geoenviron. Engng* 132(6), 817–818.

Nash, D. F. T. and Ryde, S.J. 2001. Modelling the consolidation of compressible soils subject to creep around vertical drains. *Géotechnique* 51(4), 257–273, doi: 10.1680/geot.2001.51.4.257.

Neher, H.P., Wehnert, M. and Bonnier, P.G., 2001. An evaluation of soft soil models based on trial embankments. In: C. S. Desai, ed. *Computer Methods and Advances in Geomechanics*. Rotterdam: Balkema, 373–378.

Olson, and Roy E. 1977. Consolidation under time-dependent loading. *Journal of the Geotechnical Engineering Division*, 103(1), 55–60.

Perrone, V.J. 1998. *One Dimensional Computer Analysis of Simultaneous Consolidation and Creep of Clay*. Blacksburg, Virginia.

Samson, L., and Garneau, R. 1973. Settlement performance of two embankments on deep compressible soils. Canadian Geotechnical Journal, 10(2), 211-226.

Stolle, D. F. E., Vermeer, P. A., and Bonnier, P. G. 1999. A consolidation model for a creeping clay. *Canadian Geotechnical Journal*, 36(4), 754–759.

Taylor, D. W., and Merchant, W. 1940. A theory of clay consolidation accounting for secondary compression. *Journal of Mathematics and Physics*, 19(1-4), 167–185.

Taylor, D. W. 1942. *Research on consolidation of clays*. Massachusetts Institute of Technology.

Terzaghi, K. 1943. *Theoretical Soil Mechanics*. John Wiley and Sons, New York.

Vermeer, P. A. and Neher, H. P. 1999. A soft soil model that accounts for creep. *In Beyond 2000 in computational geotechnics:10 Years of Plaxis International* (ed. R. B. J. Brinkgreve), 249–261. Rotterdam: Balkema.

Walker, R., and Indraratna B. 2009. Consolidation analysis of a stratified soil with vertical and horizontal drainage using the spectral method. *Géotechnique*, 59, 439–449.

Yin, J.-H. and Feng, W.-Q. 2017. A new simplified method and its verification for calculation of consolidation settlement of a clayey soil with creep. *Canadian Geotechnical Journal*, 54(3), 333–347.

Yin, J.-H. and Graham, J. 1989. Viscous–elastic–plastic modelling of one-dimensional time-dependent behaviour of clays. *Canadian Geotechnical Journal*, 26(2), 199–209.

Yin, J.-H. and Graham, J. 1994. Equivalent times and one-dimensional elastic viscoplastic modelling of time-dependent stress–strain behaviour of clays. *Canadian Geotechnical*

Journal, 31(1), 42–52.

Yin, J.-H., and Graham, J. 1996. Elastic visco-plastic modelling of one-dimensional consolidation. *Géotechnique*, 46(3), 515–527.

Yin, J.-H., Graham, J., Clark, J. I., and Gao, L. 1994. Modelling unanticipated pore-water pressures in soft clays. *Canadian Geotechnical Journal,* 1994, 31(5), 773–778.

Yin, J. -H., and Zhu, J.-G. 1999. Elastic viscoplastic consolidation modelling and interpretation of pore-water pressure responses in clay underneath Tarsiut Island. *Canadian Geotechnical Journal*, 36(4), 708–717.

Yin Z.Y., Karstunen M., Chang C.S., Koskinen M., Lojander M. (2011). Modeling time-dependent behavior of soft sensitive clay. *J. Geotech. Geoenviron. Eng.* ASCE, 137(11): 1103-1113.

Yin Z.Y., Jin Y.F., Shen S.L., Huang H.W. (2017). An efficient optimization method for identifying parameters of soft structured clay by an enhanced genetic algorithm and elastic-viscoplastic model. *Acta Geotech.,* 12(4): 849–867.

Yuan, Y. and Whittle, A. J. 2018. A novel elasto-viscoplastic formulation for compression behaviour of clays. *Géotechnique*, 1–12.

Zhu, G.-F. and Yin, J.-H. 1999. Consolidation of double soil layers under depth-dependent ramp load. *Géotechnique*, 49(3), 415–421.

Zhu, G.-F. and Yin, J.-H. 2005. Solution charts for the consolidation of double soil layers. *Canadian Geotechnical Journal*, 42(3), 949–956.

List of Tables

Table 1. Parameters values of Hong Kong Marine Deposits in the finite element simulations

γ_{soil} (kN/m^3)	OCR	κ^*	λ^*	μ^*	k_y (m/day)	c' (kPa)	ϕ' (°)
16	1	0.0217	0.174	0.0076 or 0.000076	1.9×10^{-4}	0.1	30

Table 2. Parameter values in the finite element simulations and the new simplified method of soil profiles in the *Skå-Edeby*

(a) Values of all parameters used in finite element simulations

Soil	γ_{soil} (kN/m^3)	OCR	POP	κ^*	λ^*	μ^*	k_y (m/day)	c' (kPa)	ϕ' (°)
Crust layer	15.46	-	100	0.04	0.1209	0.006	1.24×10^{-4}	0.1	20
Soft soil-1	15.46	1.1 or 2	-	0.04	0.1209	0.006	1.24×10^{-4}	0.1	30
Soft soil-2	16	1 or 2	-	0.059	0.098	0.0054	2.12×10^{-5}	0.1	28

(b) Values of parameters in the new simplified Hypothesis B method

Layer	e_o	γ_{soil} (kN/m^3)	C_e	C_c	$C_{\alpha e}$	k_z (m/day)	t_0 (day)
Crust layer/ Soft soil-1	2.678	15.46	0.1692	1.0227	0.0508	1.24×10^{-4}	1
Soft soil-2	2.021	16	0.4107	0.6822	0.0376	2.12×10^{-5}	1

Note POP is the pre-overburden pressure, $POP = |\sigma'_{zp} - \sigma'_z|$ λ^* is the modified compression index, $\lambda^* = \dfrac{C_c}{2.3(1+e_0)}$, κ^* is the modified swelling index, $\kappa^* \approx \dfrac{2C_e}{2.3(1+e_0)}$, μ^* is the modified creep index, $\mu^* = \dfrac{C_{\alpha e}}{2.3(1+e_0)}$.

Table 3. Parameter values in the FE modelling and the new simplified method for soil profiles in the *Berthierville* area

(a) Values of parameters in the new simplified method

Layer	e_o	γ_{soil} (kN/m^3)	C_e	C_c	$C_{\alpha e}$	k_z (m/day)	t_0 (day)
Silty clay	1.648	16	0.0656	0.811	0.009	1.5×10^{-3}	1
Sandy silt	2.021	17	0.0368	0.360	0.006	6.0×10^{-3}	1

(b) Values of all parameters used in the FE modelling

Soil	γ_{soil} (kN/m^3)	E (kN/m^2)	OCR	κ^*	λ^*	μ^*	k_y (m/day)	c' (kPa)	ϕ' (°)
Sandy layer	18	40×10^{-3}	-	-	-	-	Drained	0.1	38
Silty clay	16	1.22	1.22	0.0216	0.133	0.00148	1.5×10^{-3}	0.1	29
Sandy silt	17	1.6	1.6	0.016	0.077	0.00129	6.0×10^{-3}	0.1	32

Table 4. Summary of calculated values of parameters used in the new simplified method (*Case 2 with OCR = 1.1 for soft soil-1 and OCR = 1 for soft soil-2* as an example)

(a) Stage 1 loading

Layer i	Middle depth of sublayer (m)	$\sigma'_{z0,k}$ (kPa)	$\sigma'_{zp,k}$ (kPa)	$\sigma'_{z1,k}$ (kPa)	$\varepsilon_{zp,k}$	$\varepsilon_{f1,k}$	m_{vi} (kPa^{-1})	c_{vi} (m^2/day)
Layer 1	0.25	1.438	101.438	28.438	0.085	0.0597	0.00267	0.00473
	0.75	4.313	104.313	31.313	0.0637	0.0396		
	1.25	7.188	107.188	34.188	0.0540	0.0312		
	1.75	10.625	110.625	37.625	0.0478	0.0261		
	2.25 ~ 5.75	12.938 ~ 33.063	14.231 ~ 36.368	39.938 ~ 60.063	0.00191	0.1248 ~ 0.06065		
Layer 2	6.25 ~ 11.75	36.048 ~ 70.093	36.048 ~ 70.093	63.048 ~ 97.093	0.0	0.0548 ~ 0.0319	0.00154	0.00140

(b) Stage 2 loading

Layer i	Middle depth of sublayer (m)	$\sigma'_{z0,k}$ (kPa)	$\sigma'_{zp,k}$ (kPa)	$\sigma'_{z1,k}$ (kPa)	$\varepsilon_{zp,k}$	$\varepsilon_{f1,k}$	m_{vi} (kPa^{-1})	c_{vi} (m^2/day)
Layer 1	0.25	28.438	101.438	55.438	0.0254	0.0134	0.000371	0.0341
	0.75	31.313	104.313	58.313	0.0241	0.0124		
	1.25	34.188	107.188	61.188	0.0228	0.0116		
	1.75	37.625	110.625	64.625	0.0218	0.0109		
	2.25 ~ 5.75	39.938 ~ 60.063	65.653 ~ 98.737	66.938 ~ 87.063	0.00994	0.0123 ~ 0.00742		
Layer 2	6.25 ~ 11.75	63.048 ~ 97.093	121.858 ~ 187.660	90.048 ~ 124.093	0.01944	0.0105 ~ 0.00724	0.000322	0.00670

Table 5. Summary of calculated values of parameters used in the new simplified method (*Case* I as an example)

(a) Stage 1 loading

Layer i	Middle depth of sublayer (m)	$\sigma'_{z0,k}$ (kPa)	$\sigma'_{zp,k}$ (kPa)	$\sigma'_{z1,k}$ (kPa)	$\varepsilon_{zp,k}$	$\varepsilon_{f1,k}$	m_{vi} (kPa^{-1})	c_{vi} (m^2/day)
Layer 1	2.50	29.5	35.99	115.5	0.00215	0.15509	0.00119	0.12874
	3.00 ~ 12.00	32.5 ~ 86.5	39.65 ~ 105.53	118.5 ~ 172.5	0.00215	0.14562 ~ 0.06536		
Layer 2	12.25	88.25	141.2	174.25	0.00371	0.01624	0.00015	4.00135
	12.75 ~ 17.75	91.75 ~ 126.75	146.8 ~ 202.8	177.75 ~ 212.75	0.00371	0.01477 ~ 0.0037		

(b) Stage 2 loading

Layer i	Middle depth of sublayer (m)	$\sigma'_{z0,k}$ (kPa)	$\sigma'_{zp,k}$ (kPa)	$\sigma'_{z1,k}$ (kPa)	$\varepsilon_{zp,k}$	$\varepsilon_{f1,k}$	m_{vi} (kPa^{-1})	c_{vi} (m^2/day)
Layer 1	2.50	115.5	123.134	220.5	0.00069	0.07749	0.00063	0.23983
	3.00 ~ 12.00	118.5 ~ 172.5	126.333 ~ 183.902	223.5 ~ 277.5	0.00069	0.07588 ~ 0.05472		
Layer 2	12.25	174.25	183.796	279.25	0.00042	0.03229	0.00028	2.10986
	12.75 ~ 17.75	177.75 ~ 212.75	187.488 ~ 224.405	282.75 ~ 317.75	0.00042	0.03172 ~ 0.02685		

List of figure captions

Figure 1. Schematic diagram of multi-stage ramp loading

Figure 2. Subdivision of the multi-layer soft soils

Figure 3. The relationship between vertical strain *versus* vertical effective stress with different time lines under various stress–strain states

Figure 4. The influence of creep on the excess pore water pressure dissipation and the settlement

Figure 5. The filling loading of the embankment in Berthierville site

Figure 6. (a) Finite element simulation of soft soil layers in the *Skå-Edeby* site with three multi-stage ramp loadings (drained top and bottom); (b) finite element model of soft soil layers under the embankment of *Berthierville* site with two type loadings (drained top and impermeable bottom)

Figure 7. Comparison of vertical settlement-time curves from finite element simulations and measured data at different depths in the site of *Skå-Edeby*: (a) logarithmic scale, and (b) normal scale

Figure 8. Comparison of vertical settlement-time curves from finite element simulations and measured data in the site of *Berthierville*

Figure 9. Comparison of settlement-log(time) curves from measured data at the ground, finite element simulations, the new simplified Hypothesis B method, and the Hypothesis A method for multi-layer soils subjected to different loading conditions (*OCR = 1.1 for soft soil-1*, *OCR = 1 for soft soil-2*): (a) *Case 1,* (b) *Case 2*, and (c) *Case 3*

Figure 10. Comparison of settlement-log(time) curves from measured data at the ground, finite element simulations, the new simplified Hypothesis B method, and the Hypothesis A method for multi-layer soils subjected to different loading conditions (*OCR = 2 for soft soil-1*, *OCR = 2 for soft soil-2*): (a) *Case 1,* (b) *Case 2*, and (c) *Case 3*

Figure 11. Comparison of settlement-log(time) curves from measured data of highway embankment at *Berthierville* site, finite element simulations, the new simplified Hypothesis B method, and the Hypothesis A method for multi-layer soils subjected to different loadings: (a) Case I, (b) Case II

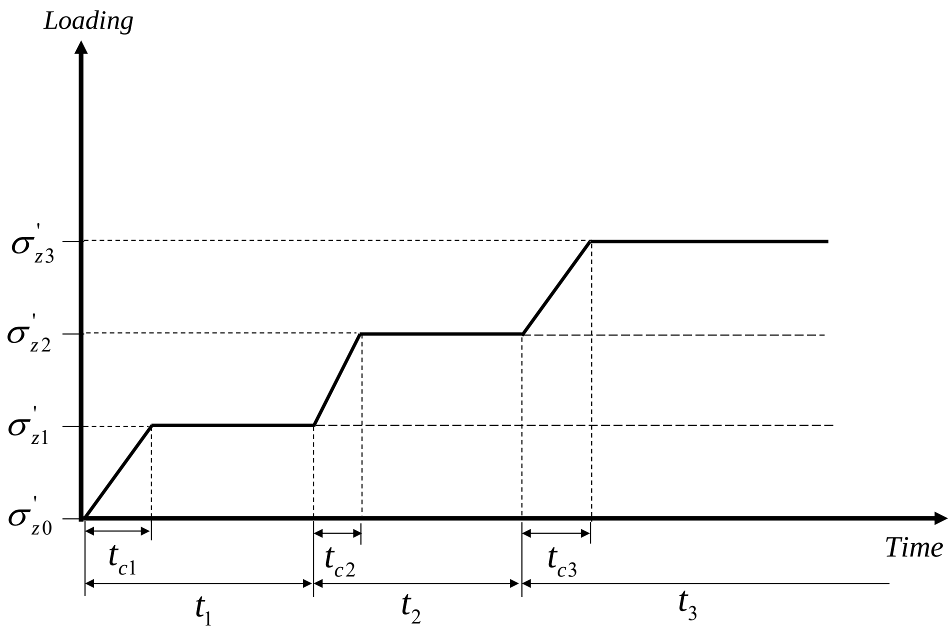

Figure 1. Schematic diagram of multi-stage ramp loading

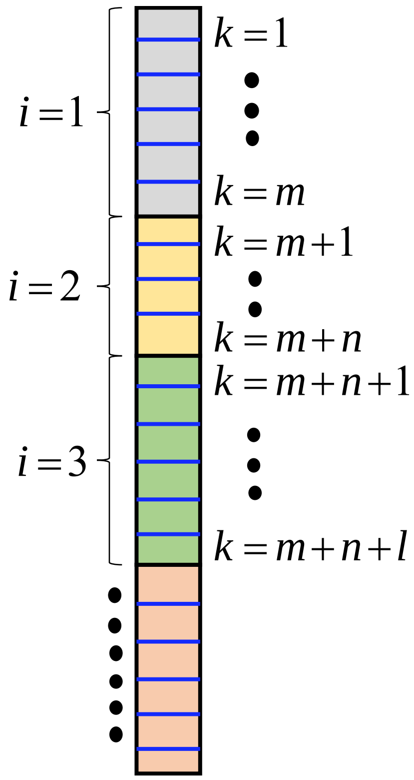

Figure 2. Subdivision of the multi-layer soft soils

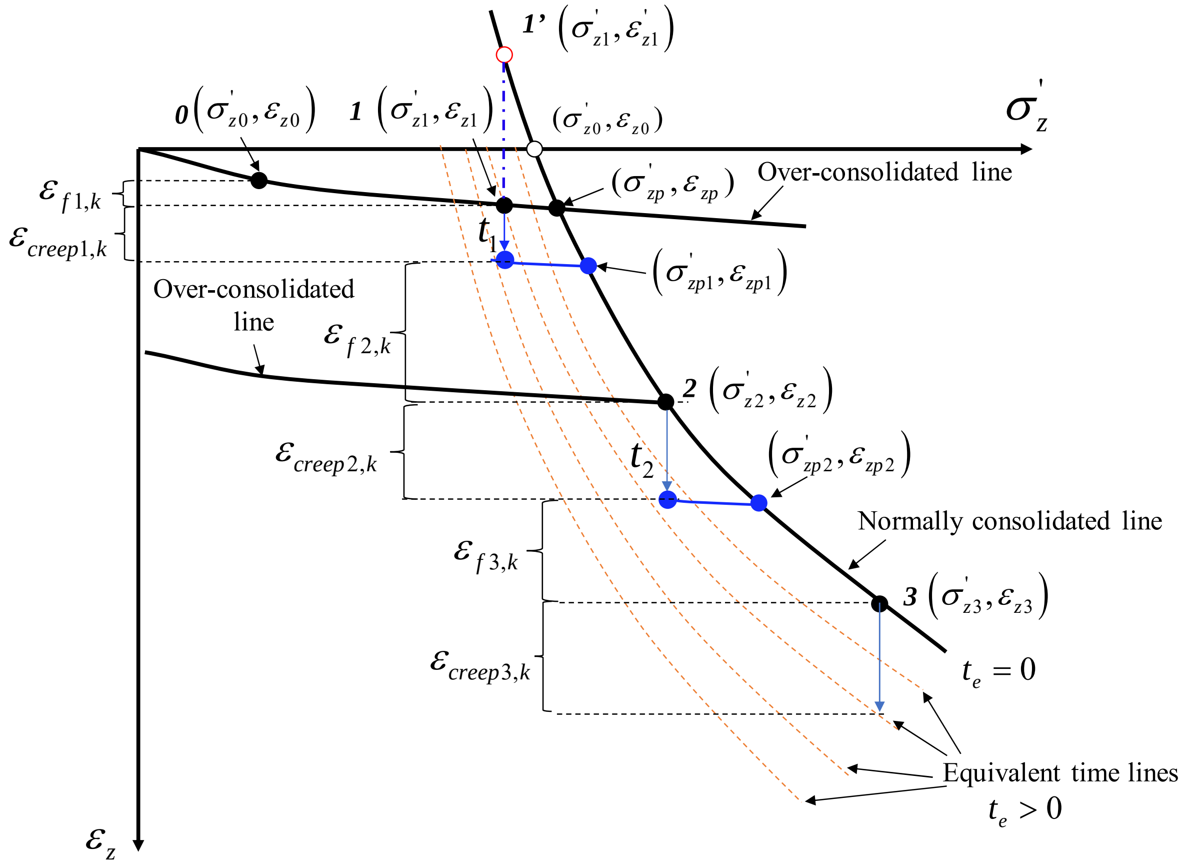

Figure 3. The relationship between vertical strain *versus* vertical effective stress with different time lines under various stress–strain states

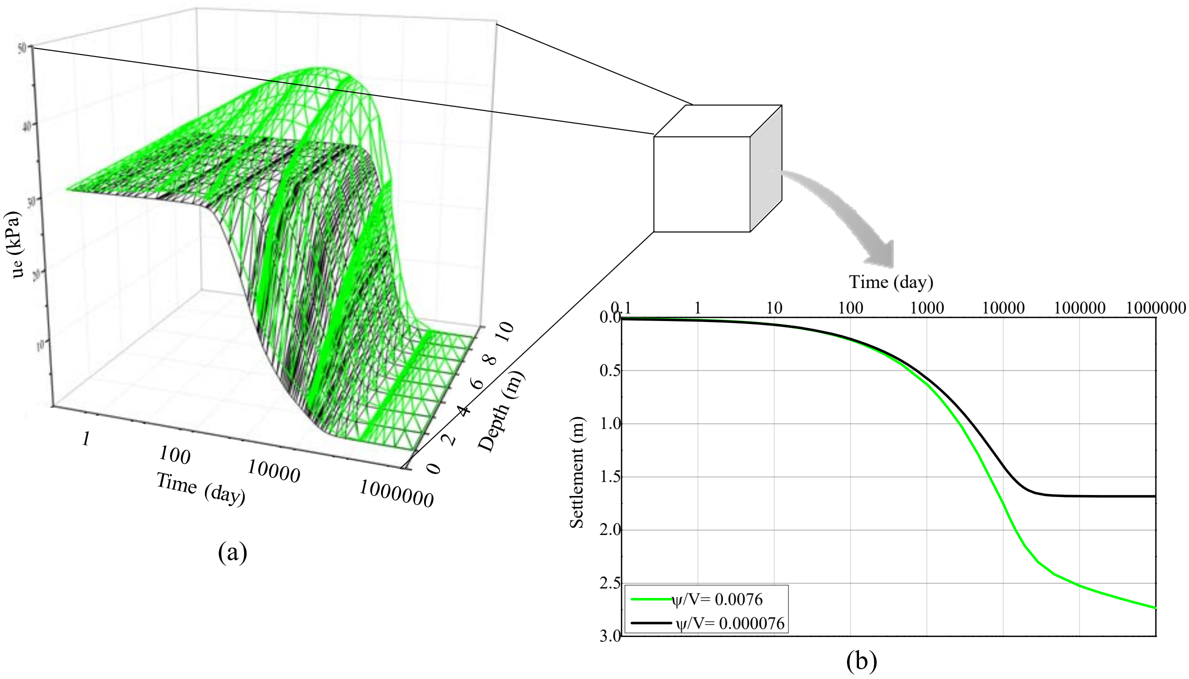

Figure 4. The influence of creep on the excess pore water pressure dissipation and the settlement

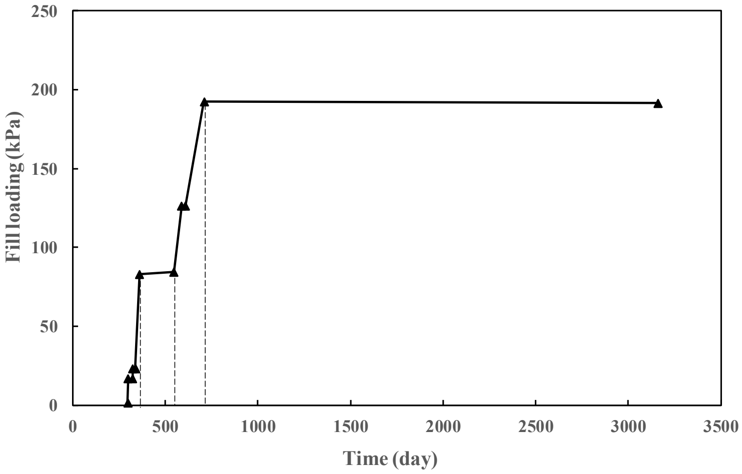

Figure 5. The filling loading of the embankment in Berthierville site

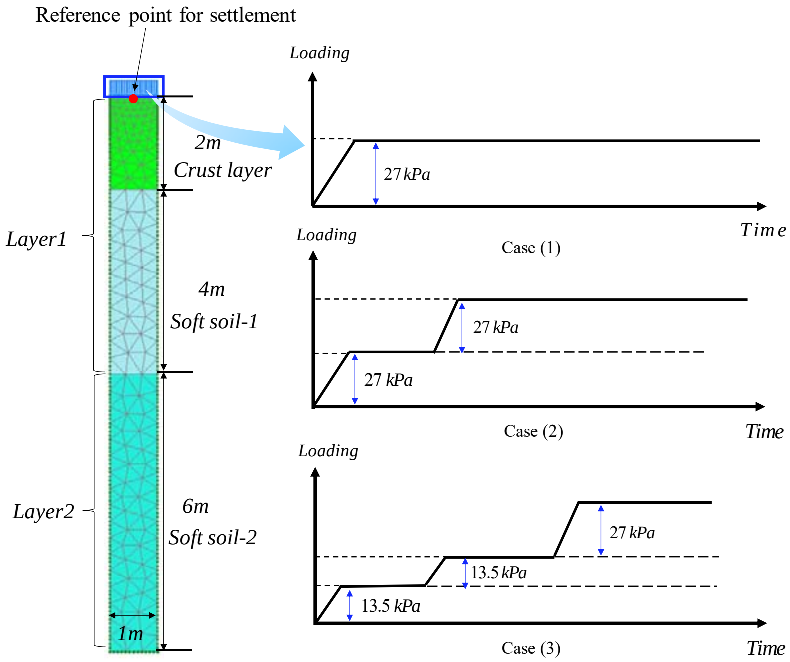

(a)

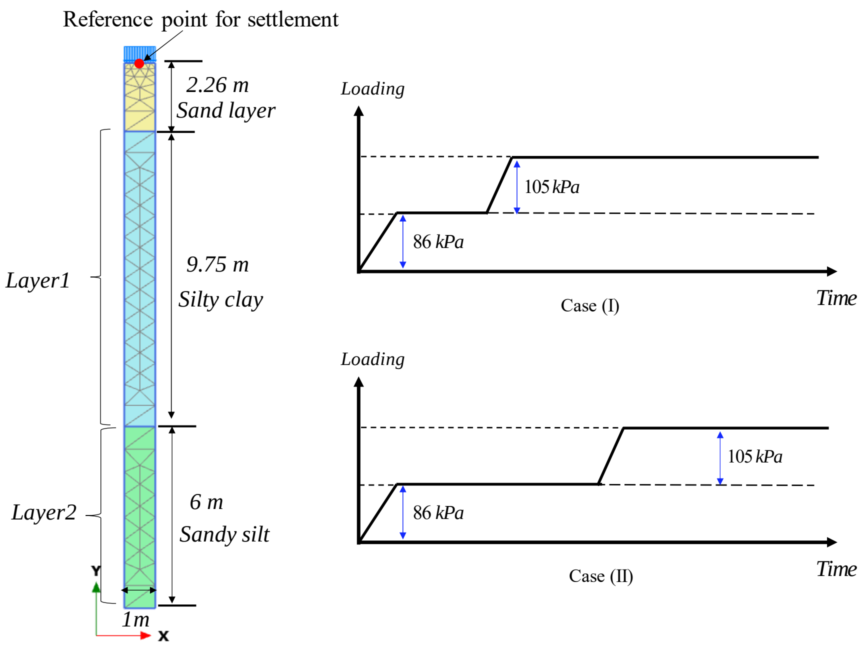

(b)

Figure 6. (a) Finite element simulation of soft soil layers in the *Skå-Edeby* site with three multi-stage ramp loadings (drained top and bottom); (b) finite element model of soft soil layers under the embankment of *Berthierville* site with two type loadings (drained top and impermeable bottom)

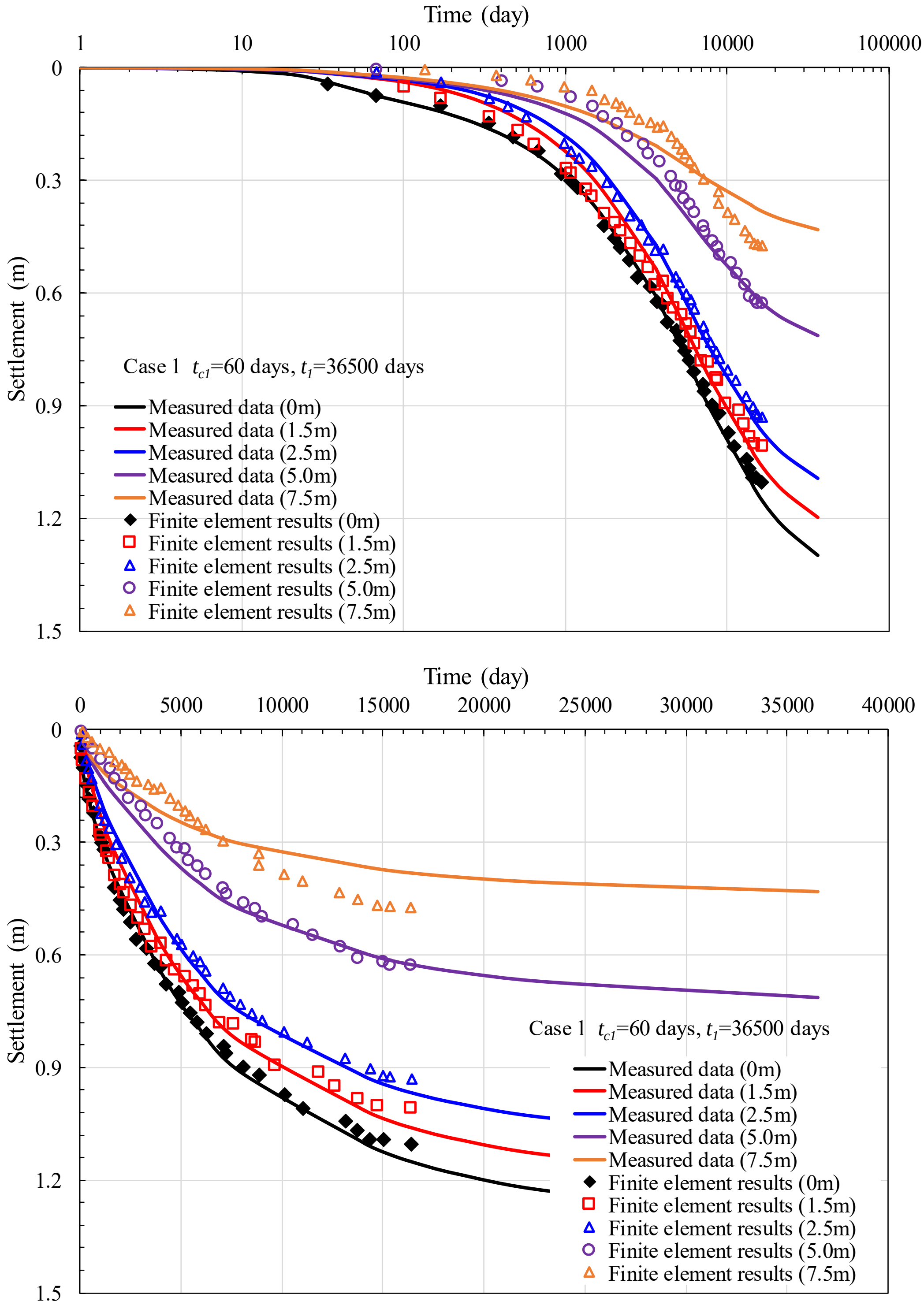

Figure 7. Comparison of vertical settlement-time curves from finite element simulations and measured data at different depths in the site of *Skå-Edeby*: (a) logarithmic scale, and (b) normal scale

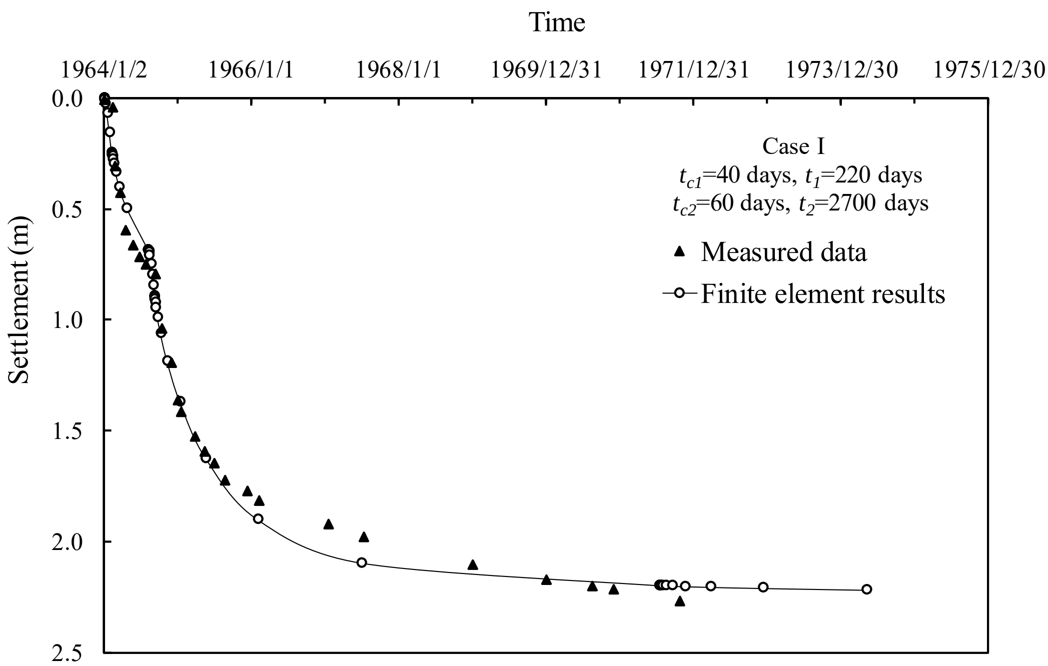

Figure 8. Comparison of vertical settlement-time curves from finite element simulations and measured data in the site of *Berthierville*

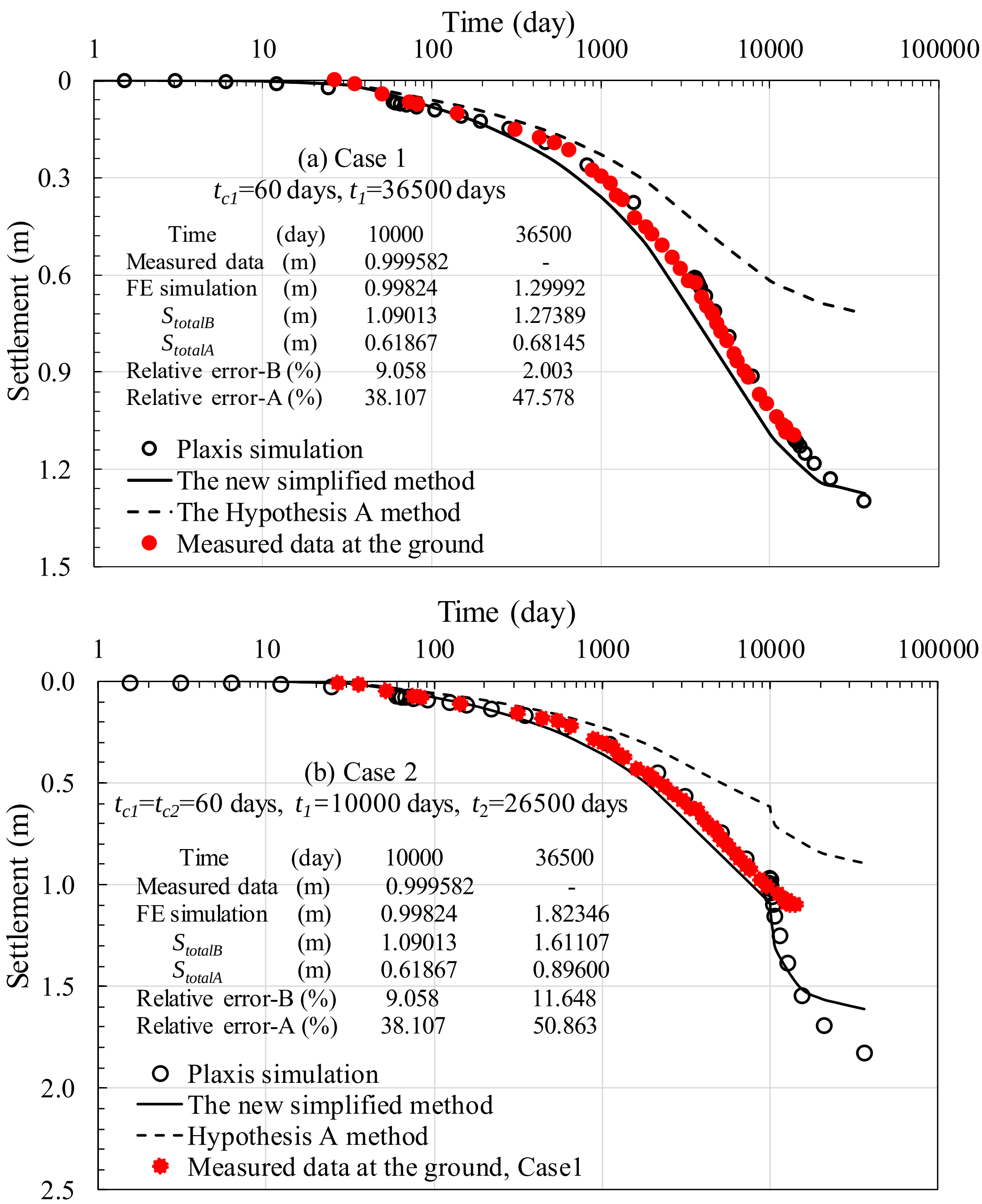

Time (day)
1
10
100
1000
10000
100000
0
0.3
0.6
0.9
1.2
1.5
Settlement (m)
(a) Case 1
t_{c1}=60 days, t_1=36500 days
Time (day) 10000 36500
Measured data (m) 0.999582 -
FE simulation (m) 0.99824 1.29992
S_{totalB} (m) 1.09013 1.27389
S_{totalA} (m) 0.61867 0.68145
Relative error-B (%) 9.058 2.003
Relative error-A (%) 38.107 47.578
Plaxis simulation
The new simplified method
The Hypothesis A method
Measured data at the ground
Time (day)
1
10
100
1000
10000
100000
0.0
0.5
1.0
1.5
2.0
2.5
Settlement (m)
(b) Case 2
t_{c1}=t_{c2}=60 days, t_1=10000 days, t_2=26500 days
Time (day) 10000 36500
Measured data (m) 0.999582 -
FE simulation (m) 0.99824 1.82346
S_{totalB} (m) 1.09013 1.61107
S_{totalA} (m) 0.61867 0.89600
Relative error-B (%) 9.058 11.648
Relative error-A (%) 38.107 50.863
Plaxis simulation
The new simplified method
Hypothesis A method
Measured data at the ground, Case1

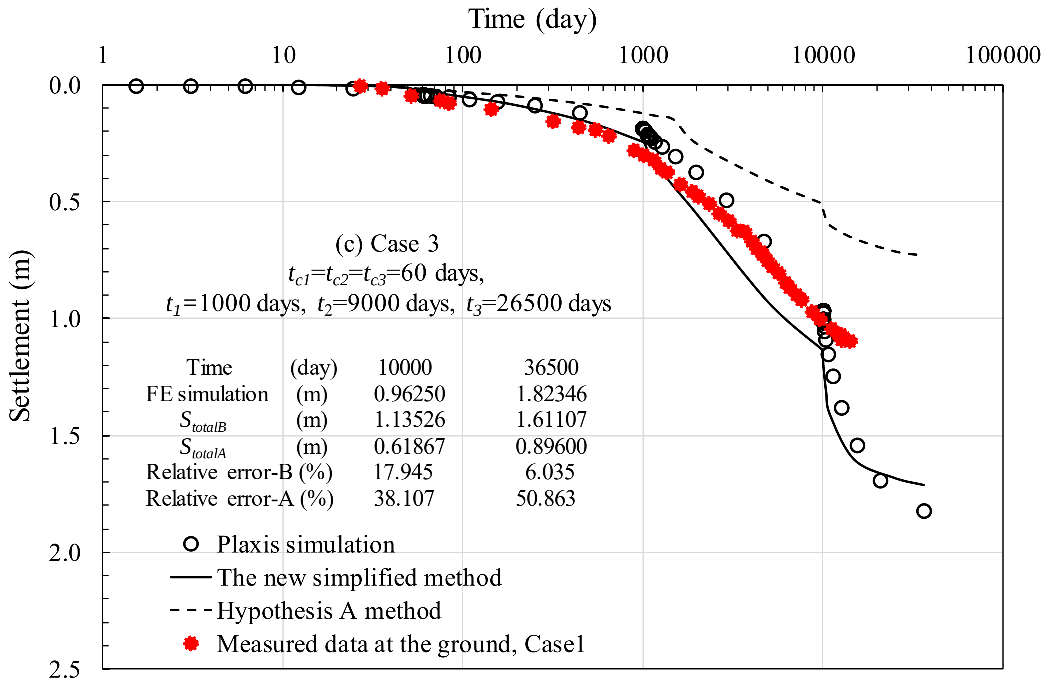

Figure 9. Comparison of settlement-log(time) curves from measured data at the ground, finite element simulations, the new simplified Hypothesis B method, and the Hypothesis A method for multi-layer soils subjected to different loading conditions (*OCR = 1.1 for soft soil-1*, *OCR = 1 for soft soil-2*): (a) *Case 1*, (b) *Case 2*, and (c) *Case 3*

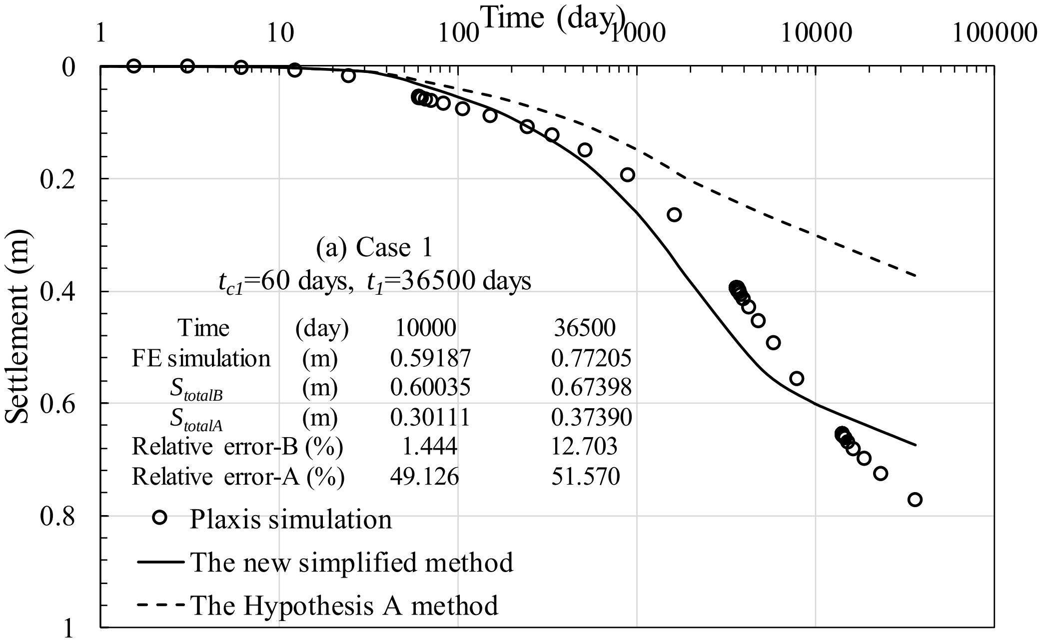
Time (day)
1
10
100
1000
10000
100000
0
0.2
0.4
0.6
0.8
1
Settlement (m)
(a) Case 1
t_{c1}=60 days, t_1=36500 days
Time (day) 10000 36500
FE simulation (m) 0.59187 0.77205
S_{totalB} (m) 0.60035 0.67398
S_{totalA} (m) 0.30111 0.37390
Relative error-B (%) 1.444 12.703
Relative error-A (%) 49.126 51.570
Plaxis simulation
The new simplified method
The Hypothesis A method

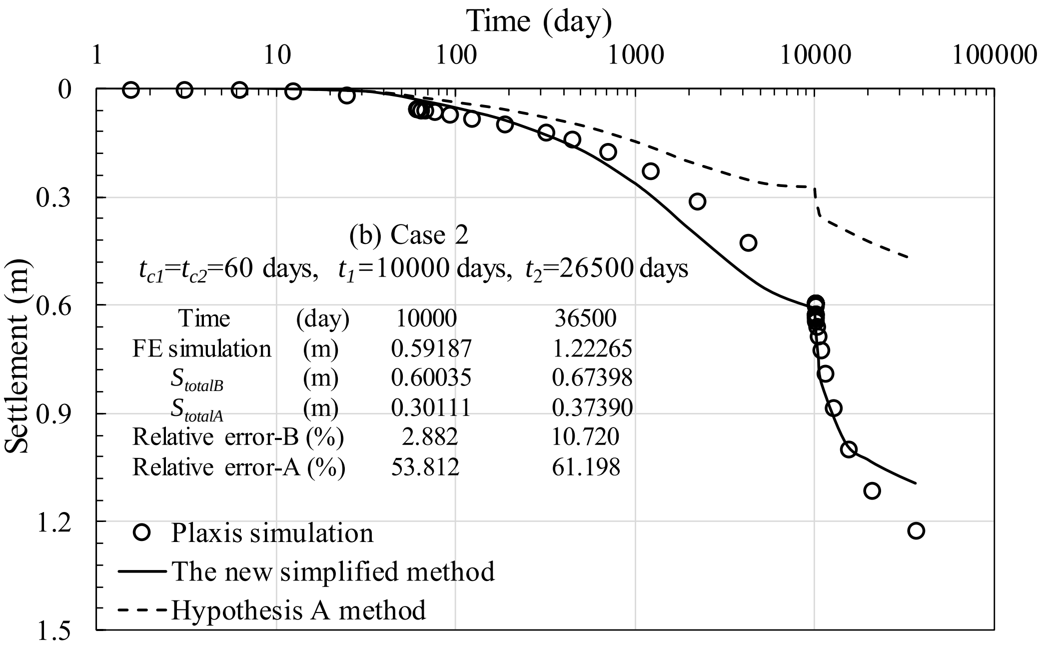
Time (day)
1
10
100
1000
10000
100000
0
0.3
0.6
0.9
1.2
1.5
Settlement (m)
(b) Case 2
t_{c1}=t_{c2}=60 days, t_1=10000 days, t_2=26500 days
Time (day) 10000 36500
FE simulation (m) 0.59187 1.22265
S_{totalB} (m) 0.60035 0.67398
S_{totalA} (m) 0.30111 0.37390
Relative error-B (%) 2.882 10.720
Relative error-A (%) 53.812 61.198
Plaxis simulation
The new simplified method
Hypothesis A method

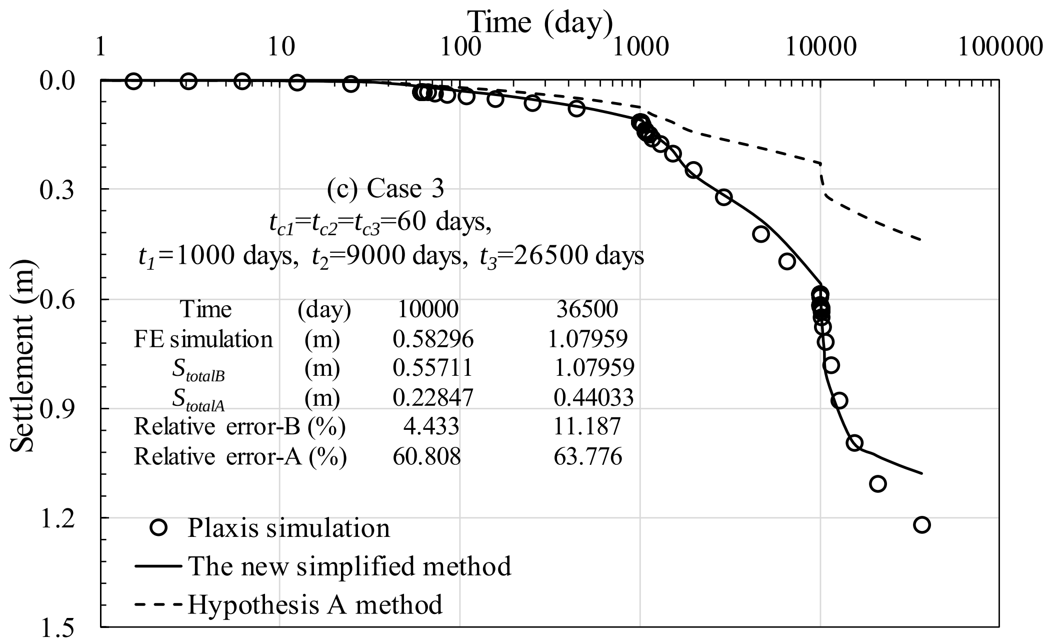

Figure 10. Comparison of settlement-log(time) curves from measured data at the ground, finite element simulations, the new simplified Hypothesis B method, and the Hypothesis A method for multi-layer soils subjected to different loading conditions (*OCR = 2 for soft soil-1*, *OCR = 2 for soft soil-2*): (a) *Case 1,* (b) *Case 2*, and (c) *Case 3*

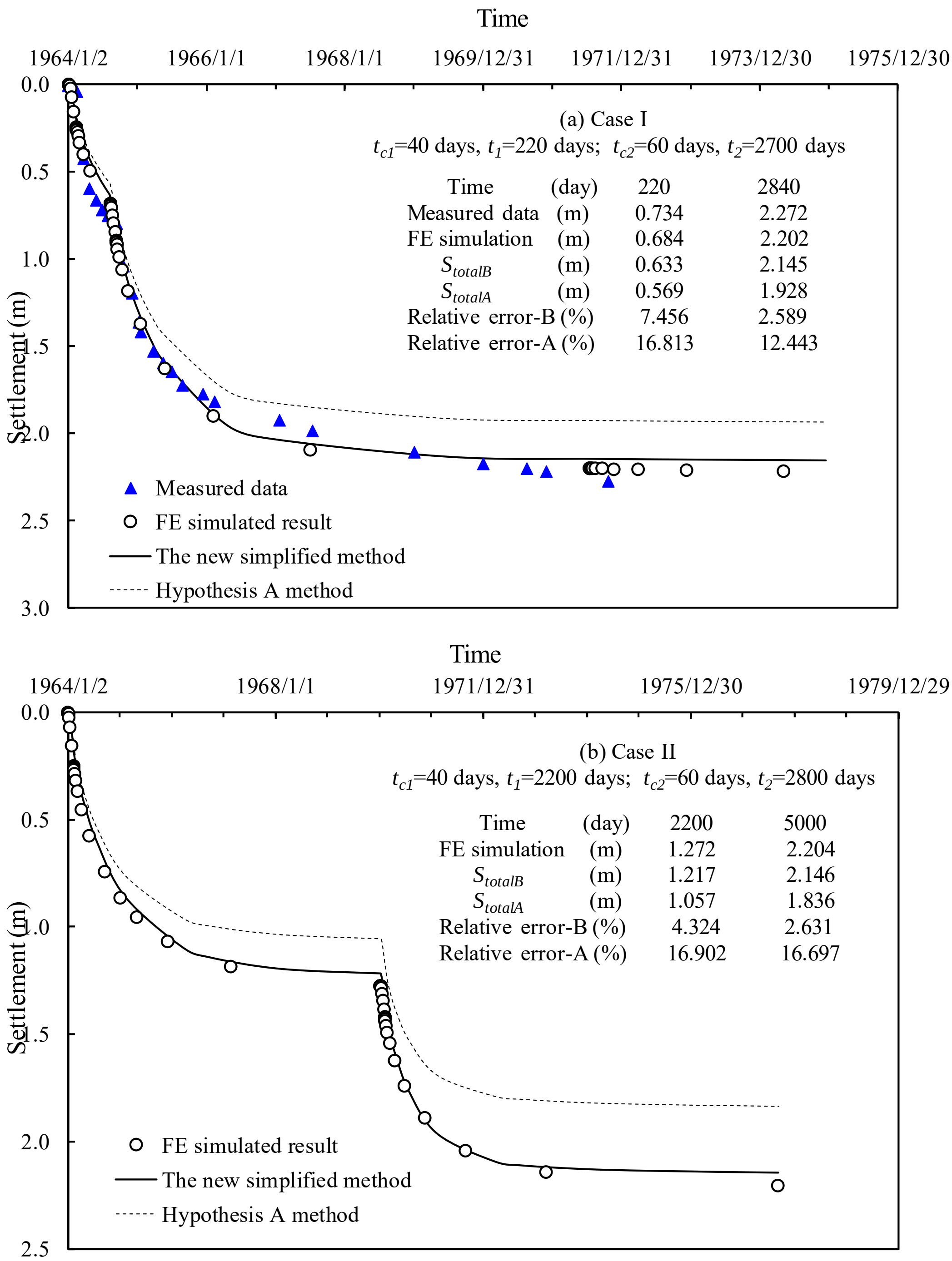

Figure 11. Comparison of settlement-log(time) curves from measured data of highway embankment at *Berthierville* site, finite element simulations, the new simplified Hypothesis B method, and the Hypothesis A method for multi-layer soils subjected to different loadings: (a) Case I, (b) Case II